Structures, Stabilities, and Electronic and Optical Properties of C_{62} Fullerene Isomers

Yan-Hong Cui,[†] De-Li Chen,[†] Wei Quan Tian,*[,†] and Ji-Kang Feng*[,†,‡]

State Key Laboratory of Theoretical and Computational Chemistry, Institute of Theoretical Chemistry, Jilin University, Changchun 130023, China, and College of Chemistry, Jilin University, Changchun 130023, China

Received: April 9, 2007; In Final Form: May 29, 2007

The 2385 classical isomers and four nonclassical isomers of fullerene C_{62} have been studied by PM3, HCTH/3-21G//SVWN/STO-3G, B3LYP/6-31G(d)//HCTH/3-21G, and B3LYP/6-31G(d)//B3LYP/6-31G(d). The C_s:7*mbr* isomer, with a chain of four adjacent pentagons surrounding a heptagon, is predicted to be the most stable isomer, followed by C_{2v}:4*mbr* which is 3.15 kcal/mol higher in energy. C_2:0032 with three pairs of adjacent pentagons is the most stable isomer in the classical framework. To clarify the relative stabilities of C_{62} isomers at high temperatures, the entropy contributions are taken into account on the basis of the Gibbs energy at the B3LYP/6-31G(d) level. Analyses reveal that C_s:7*mbr* prevails in a wide temperature range. The vibrational frequencies of the five most stable C_{62} fullerene isomers are also predicted at the B3LYP/6-31G(d) level, and the simulated IR spectra show important differences in positions and intensities of the vibrational modes for different isomers. The nucleus-independent chemical shift and the density of states of the three most stable isomers show that the square in C_{2v}:4*mbr* and the adjacent pentagons in C_s:7*mbr* and C_2:0032 possess high chemical reactivity. In addition, the electronic spectra and second-order hyperpolarizabilities are determined by means of ZINDO and the sum-over-states mode. The intensity-dependent refractive index $\gamma(-\omega; \omega, \omega, -\omega)$ at $\omega = 2.3305$ eV of C_s:7*mbr* is very large because of resonance with the external field. The second-order hyperpolarizabilities of the five most stable isomers of C_{62} are predicted to be larger than those of C_{60}.

1. Introduction

Since the discovery[1] of the buckminsterfullerene C_{60}, along with its macroscopic scale synthesis,[2] fullerene study as an interdisciplinary field has attracted extensive attention.[3,4] The search for other fullerenes has been an active research area, resulting in much success for C_{60} and higher fullerenes. With increasing size, however, the number of isomers rapidly multiplies, and as a consequence of steric strain and the high-temperature conditions of isomer formation, only pure "classical" fullerene isomers with pentagons and hexagons have been successfully isolated. In fact, most of the experimentally isolated fullerenes are part of a subset having nonadjacent pentagons, a fact known as the isolated-pentagon rule (IPR).[5−7] According to this empirical rule, C_{70} is the first fullerene that is "stable" after C_{60} because the intermediate fullerenes $C_{62}-C_{68}$ include energetically unfavorable fusion of two pentagons within their structures. For C_{62}, three non-IPR isomers with minimal strain have been proposed,[5] and one nonclassical structure with fused square−pentagon units was also predicted to possess low energy.[8−11] Another nonclassical isomer with heptagon−hexagon units with even lower energy has also been predicted.[12,13] Recently, Hou et al. studied the dimerization of square−pentagonal C_{62}, H_2-C_{62}, and F_2-C_{62}.[14]

C_{62} has 2385 isomers obeying the classical definitions with only pentagons and hexagons,[5] three of which have the smallest number of e_{55} ($e_{55} = 3$): the number of pentagon−pentagon fusions.[15] A C_{2v}-symmetric C_{62} with one square was recently proposed,[13] and the successful synthesis of its stable derivative (4-Me-$C_6H_4)_2$-C_{62} indicated that nonclassical fullerenes with a square can exist. The nonclassical C_{62} fullerene with a heptagonal ring was investigated by Ayuela et al.[8] The nonclassical C_{62} fullerenes and derivatives from C_{60} are of general interest because of their close connection with the most abundant fullerene C_{60}. To our best knowledge, a systematic theoretical study on C_{62} fullerenes is absent, although a few investigations have been reported.[5,8−15] Therefore, full geometry optimizations of all classical and some nonclassical isomers of C_{62} are carried out in this study. To evaluate the temperature-dependent relative stabilities of C_{62} isomers, entropy contributions are taken into account on the basis of the Gibbs function under the condition of interisomeric thermodynamic equilibrium. Finally, calculations are also performed for IR spectra, nucleus-independent chemical shift (NICS), UV−vis spectra, and nonlinear optical (NLO) properties for several of the most stable C_{62} isomers.

2. Computational Details

The geometry optimizations of all 2385 classical isomers generated with the FULLGEN program,[16] along with four nonclassical isomers of C_{62} fullerene, are performed first with the semiempirical method PM3.[17] The geometries of the 81 most stable classical isomers from PM3, with relative energies within 50 kcal/mol, are refined with HCTH[18]/3-21G//SVWN[19]/STO-3G. All geometries of the first 24 most stable isomers from HCTH/3-21G//SVWN/STO-3G are refined with B3LYP[20]/6-31G(d)//HCTH/3-21G and B3LYP/6-31G(d)//B3LYP/6-31G(d). HCTH/3-21G is chosen in geometry optimization for C_{62} due to its good performance in C_{50}, C_{60}, and C_{70} geometry optimizations[21] and inclusion of gradient fitting in the HCTH

* E-mail: tianwq@jlu.edu.cn.
[†] State Key Laboratory of Theoretical and Computational Chemistry, Jilin University.
[‡] College of Chemistry, Jilin University.

10.1021/jp072768c CCC: $37.00
Published on Web 07/13/2007

functionals.[18] All geometry optimizations are carried out within the Gaussian 03 quantum chemical package.[22]

Upon the optimized structures predicted by B3LYP/6-31G-(d) are carried out the harmonic vibrational analyses at the same level of theory for the five most stable isomers of C_{62}. Rotational−vibrational partition functions are constructed from the optimized structural and the vibrational frequencies with rigid rotator and harmonic oscillator approximations, and no frequency scaling is performed. Relative concentrations (mole fractions), x_i, of the ith isomer among the m isomers can be expressed through the partition functions q_i and the ground-state energies $\Delta H^\circ_{0,i}$ by a compact formula:[23]

$$x_i = \frac{q_i \exp[-\Delta H^\circ_{0,i}/(RT)]}{\sum_{j=1}^{m} q_j \exp[-\Delta H^\circ_{0,j}/(RT)]} \quad (1)$$

where R is the gas constant and T is the absolute temperature. Equation 1 refers to the relative ground-state energies $\Delta H^\circ_{0,i}$, i.e., the enthalpies at the absolute zero temperature. Hence, the conventional heats of formation at room temperature $\Delta H^\circ_{f,298}$ in our calculations are converted to the heats of formation at the absolute zero temperature $\Delta H^\circ_{f,0}$. It is necessary to stress that eq 1 is an exact formula that can be directly derived from the standard Gibbs energies of the isomers, and it is strongly temperature-dependent.[23] The chirality contribution is not considered in our study.

Upon the optimized structures predicted by B3LYP/6-31G-(d) are carried out the NICS analyses at the same level of theory for the three most stable isomers. In addition, we perform ZINDO calculations on the electronic spectra for the five most stable C_{62} isomers. The reliability of the ZINDO method has been verified.[24−26] The UV−vis spectra and the second-order hyperpolarizabilities are predicted by ZINDO/SCI[27] in combination with the sum-over-states (SOS) scheme.[28,29] In the UV−vis spectra and second-order hyperpolarizabilities (γ) calculations, an active space of 28 occupied and 28 virtual orbitals (784 single-electron excitation configurations) plus the ground state are included. These calculations are performed upon the B3LYP/6-31G(d) optimized geometries.

3. Results and Discussions

3.1. Relative Energies and Structures of C_{62} Isomers. The structures of the 24 most stable isomers in energetic order are shown in Figure 1, and the relative energies predicted by several methods are listed in Table 1. The numeric indices of the C_{62} classical isomers follow their order of appearance within each distinct symmetry from FULLGEN.

The relative energies of the 24 C_{62} isomers from PM3, HCTH/3-21G//SVWN/STO-3G, B3LYP/6-31G(d)//HCTH/3-21G, and B3LYP/6-31G(d)//B3LYP/6-31G(d) are listed in Table 1. B3LYP/6-31G(d)//B3LYP/6-31G(d) predicts the isomer labeled as C_s:7*mbr*, with a heptagon, to be the most stable isomer for C_{62}, and the second most stable isomer was predicted to be C_{2v}:4*mbr* with a square that is 3.15 kcal/mol higher in energy. The two most stable isomers of C_{62} are, surprisingly, nonclassical fullerenes, which are heptagon-containing or square-containing fullerene isomers. Both of them are formed through a C2-unit addition into fullerene C_{60} (See Scheme 1). Isomer C_s:7*mbr* is formally a product of a C2-unit insertion into a hexagonal face of C_{60}, which has been described by Ayuela et al.[8] (shown in Scheme 1A). The conceptual approach to C_{2v}:4*mbr* with a square ring is obtained by insertion of a C2-unit into two adjacent 5,6-ring junctions of C_{60} fullerene as described by Qian et al.[13] (shown in Scheme 1B). The third most stable isomer C_2:0032 which possesses the lowest energy among the classical isomers is about 13.52 kcal/mol higher in energy than C_s:7*mbr*. The classical isomers C_1:0899 and C_1:1077 possess slightly higher energies than that of C_2:0032, i.e., 0.75 kcal/mol and 2.43 kcal/mol higher in energy, respectively, while the other C_{62} isomers are at least 11.07 kcal/mol higher in energy than C_2:0032. We should note that C_1:7+4 is another nonclassical isomer by inserting a C2-unit into an adjacent 6,6-ring junction of C_{60} (see Scheme 1C). The C_1:7+4 is 21.12 kcal/mol higher in energy than C_s:7*mbr*, and another nonclassical isomer is not listed due to its very high relative energy.

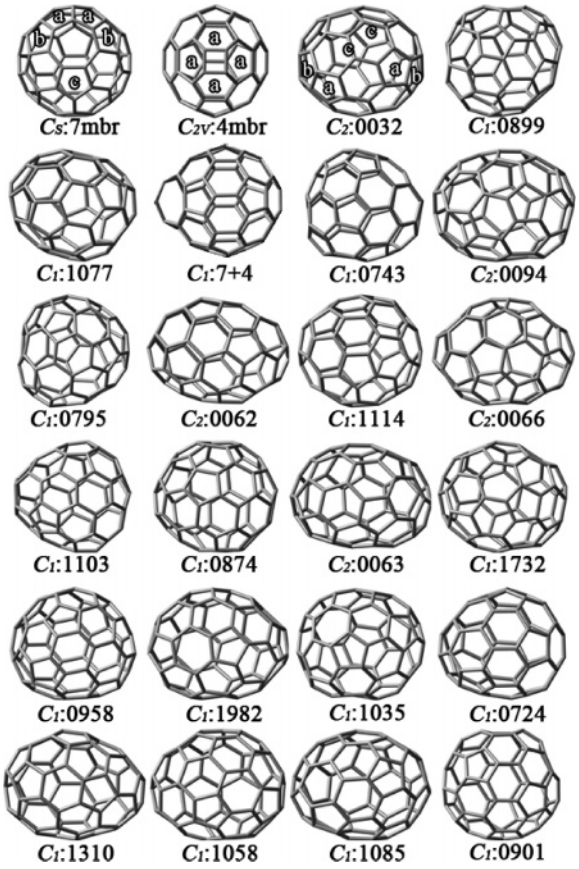

Figure 1. Structures of the first 24 most stable isomers of C_{62}.

The order of relative energies obtained with PM3 is distinctly different from that based on B3LYP/6-31G(d)//B3LYP/6-31G-(d), with the largest difference of 25.84 kcal/mol. The order of relative energies for the 24 isomers predicted by B3LYP/6-31G-(d)//HCTH/3-21G agrees well with that based on B3LYP/6-31G(d)//B3LYP/6-31G(d). The order of a few isomers varies (as listed in Table 1), and the largest difference of relative energies (ΔE_{rel}) obtained by these two methods is less than 3.74 kcal/mol. In addition, the order of relative energies predicted by HCTH/3-21G//HCTH/3-21G is slightly different from that based on B3LYP/6-31G(d)//HCTH/3-21G, with the largest ΔE_{rel} less than 8.02 kcal/mol. These results suggest that the B3LYP/6-31G(d)//HCTH/3-21G method predicts the relative energies better than those from the HCTH/3-21G//HCTH/3-21G method, supporting B3LYP/6-31G(d)//HCTH/3-21G as a reliable and efficient approximation for fullerene geometry and relative energy prediction.[21]

The gap between the highest occupied molecular orbital and the lowest unoccupied molecular orbital (HOMO−LUMO) and

TABLE 1: Relative Energies of C_{62} Isomers from PM3, HCTH/3-21G//SVWN/STO-3G, B3LYP/6-31G(d)//HCTH/3-21G, and B3LYP/6-31G(d)[a]

	e_{55}[b]	PM3	HCTH/3-21G //SVWN/STO-3G	B3LYP/6-31G(d) //HCTH/3-21G	B3LYP/6-31G(d) //B3LYP/6-31G(d)	ΔE_{gap}[c]
C_s:7*mbr*	3	1.61	0.00 (0.00)	0.00 (0.00)	0.00	1.38
C_{2v}:4*mbr*	0	0.00	5.37 (5.77)	3.30 (5.55)	3.14	1.84
C_2:0032	3	16.27	10.47 (11.61)	13.81 (10.63)	13.52	1.28
C_1:0899	3	17.77	10.25 (11.58)	14.53 (10.31)	14.27	1.12
C_1:1077	4	12.95	13.02 (15.21)	16.24 (12.96)	15.95	1.26
C_1:7+4	0	21.98	24.10 (28.46)	22.05 (25.02)	21.12	1.82
C_1:0743	4	26.23	21.52 (24.31)	25.03 (21.40)	24.59	1.65
C_2:0094	4	33.16	20.39 (23.85)	25.40 (20.35)	24.91	1.49
C_1:0795	4	29.13	24.24 (27.56)	28.17 (23.99)	27.66	1.38
C_2:0062	4	53.64	20.48 (27.48)	28.02 (20.40)	27.80	1.25
C_1:1114	4	35.30	25.12 (27.74)	30.08 (25.08)	29.53	1.30
C_2:0066	4	32.37	22.14 (30.14)	29.93 (21.91)	29.65	2.08
C_1:1103	4	29.97	25.65 (29.68)	30.21 (25.57)	29.76	1.51
C_1:0874	4	37.25	26.10 (28.81)	30.59 (25.99)	30.05	1.40
C_2:0063	4	34.03	25.54 (30.95)	31.75 (25.33)	31.27	1.83
C_1:1732	4	44.01	27.65 (32.19)	33.59 (27.46)	31.43	1.29
C_1:0958	4	32.03	27.57 (31.99)	32.06 (27.37)	31.62	1.48
C_1:1982	4	45.93	24.64 (31.62)	32.07 (24.52)	31.70	1.28
C_1:1035	4	51.83	26.85 (30.76)	32.88 (26.77)	32.44	1.06
C_1:0724	4	34.73	28.84 (33.27)	33.33 (28.69)	32.80	1.46
C_1:1310	4	40.33	27.61 (33.65)	34.18 (27.47)	33.97	1.46
C_2:0061	4	55.90	27.22 (34.66)	34.85 (27.25)	34.58	1.07
C_1:1085	4	42.14	29.27 (34.51)	34.42 (29.12)	35.71	0.95
C_1:1058	4	45.38	27.96 (33.27)	34.73 (27.90)	36.18	1.13
C_1:0901	4	54.31	29.15 (34.62)	35.40 (28.97)	39.14	1.34

[a] The values in parentheses of the HCTH/3-21//SVWN/STO-3G and B3LYP/6-31G(d)//HCTH/3-21G columns are obtained from SVWN/STO-3G and HCTH/3-21G, respectively. The relative energies are in kcal mol^{-1}, and the HOMO−LUMO gaps (ΔE_{gap}) are in eV. [b] e_{55}: the number of pentagon−pentagon fusions. [c] ΔE_{gap}: predicted by B3LYP/6-31G(d) based on the B3LYP/6-31G(d) geometries.

SCHEME 1: Conceptual Formation of C_s:7*mbr*, C_{2v}:4*mbr*, and C_1:7+4 by Insertion of a C2-Unit into C_{60}

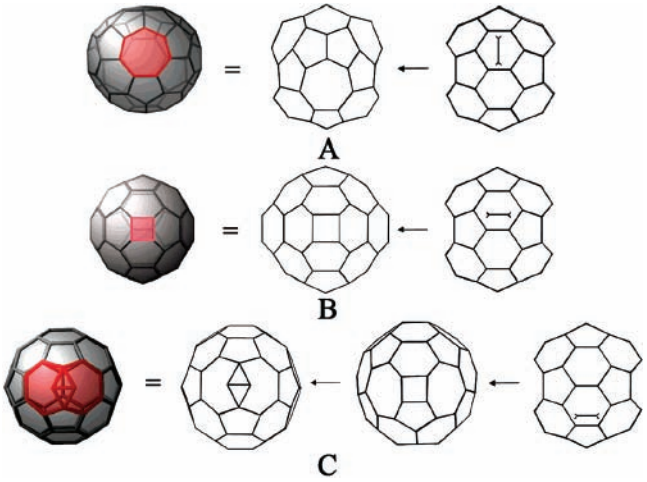

the e_{55} of each isomer are also listed in Table 1. The HOMO−LUMO gap for the most stable isomer C_s:7*mbr* is 1.38 eV predicted by B3LYP/6-31G(d), while the HOMO−LUMO gap does not necessarily correlate with the relative stability of fullerene isomers as shown in Table 1. C_{2v}:4*mbr* has a larger HOMO−LUMO gap of 1.84 eV than that of C_s:7*mbr*.

Ayuela et al. described[8] that stability of fullerenes with a heptagon is found to increase with e_{57}, the number of pentagon−heptagon fusions: a simple recipe for the low-energy structure is therefore to minimize e_{55} and then maximize e_{57}. These trends suggest that a nonclassical fullerene might overtake the classical structures in stability for some nuclearity where e_{55} cannot be zero while e_{57} may be large for the minimal value of e_{55}. Therefore, it is not surprising that the most stable isomer of C_{62} is the C_s:7*mbr* isomer with a chain of four adjacent pentagons surrounding a heptagon.

The observed fullerenes belong to the subset of classical isomers with isolated pentagons, which is only possible for cages C_{ns} with $n = 60$ or $n = 70 + 2k$ for $k \geq 0$. In those cases where is impossible to have all the pentagons isolated in a fullerene cage, the most stable isomer corresponds to the situation in which e_{55} is as low as possible. This second rule is known as the pentagon adjacency penalty rule (PAPR).[15] According to the PAPR, the isomer with the lowest e_{55} should be the most stable isomer, and the most stable classical isomer (C_2:0032) indeed possesses the lowest e_{55} ($e_{55} = 3$) value among the classical isomers. In addition, as for the classical isomers, the energetic costs are found to increase with the value of e_{55}. Hence, the sequence of relative energy for the classical isomers is well explained with the PAPR.

3.2. Relative Concentration of C_{62} Isomers. Energetics itself cannot predict relative stabilities in an isomeric system, especially at high temperatures, as stability interchange induced by the enthalpy−entropy interplay is possible. This situation is particularly pertinent to fullerene; hence, we include entropic effects and evaluate the relative concentrations through the Gibbs free energy at the B3LYP/6-31G(d) level of theory up to 4000 K. Considering the high computational cost of these calculations, only the five most stable isomers with relative energies within 20 kcal/mol are considered for equilibrium statistical thermodynamic analyses in the present study. In Figure 2, the temperature evolution of the concentrations of C_{62} isomers has been evaluated in order to gain a deeper insight into the relative stability of C_{62} isomers at different temperatures. It turns out that the nonclassical C_s:7*mbr* isomer prevails in the whole temperature interval considered. Hence, the C_s:7*mbr* isomer should be more thermodynamically stable than other isomers over a wide range of temperatures. As shown in Figure 2, another nonclassical isomer C_{2v}:4*mbr* is also an important component and reaches its maximum at around 2600 K. In addition, it should be mentioned that the classical C_1:0899

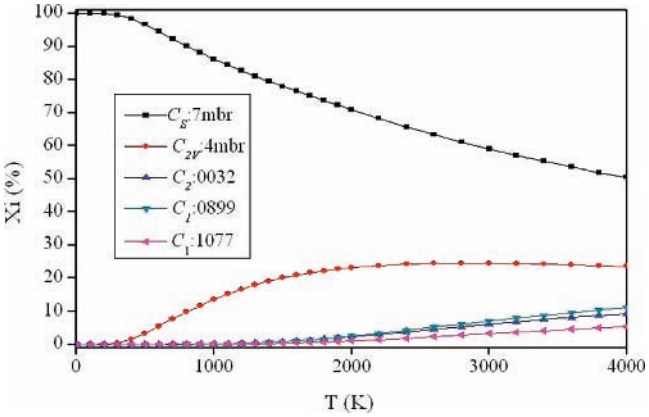

Figure 2. B3LYP/6-31G(d) relative concentrations of the five most stable C_{62} isomers.

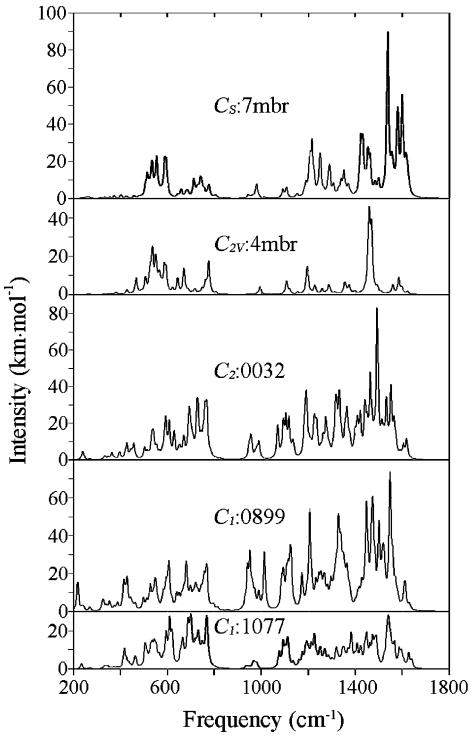

Figure 3. Simulated IR spectra for the five most stable isomers of C_{62}.

isomer surpasses the classical C_2:0032 isomer around 2000 K; however, all of the classical isomers possess low relative concentration. In conclusion, the results show that C_s:7*mbr* should be the dominant component during the generation of C_{62} and the classical isomers are less favored.

3.3. Infrared Spectra. We also evaluate the harmonic vibrational frequencies for the five most stable isomers within 20 kcal/mol based on the B3LYP/6-31G(d) prediction, and the simulated IR spectra are presented in Figure 3. All the IR spectra can be divided into two regions: the first one (from 1000 to 1600 cm^{-1}) corresponds to the C−C stretching modes and the second one (from 300 to 800 cm^{-1}) mainly corresponds to the breathing modes of the cages. Some main features of the spectra are summarized as below. First, among the breathing modes, the most stable classical isomer (C_2:0032) presents the most intensive peak at 691 cm^{-1}, and C_{2v}:4*mbr* shows the weakest peaks compared to the other four isomers. Second, the most stable isomer (C_s:7*mbr*) shows the most intensive peak in the region of C−C stretching mode (e.g., 1538 cm^{-1}). The peak (1538 cm^{-1}) corresponds to the stretching of C−C bonds of adjoined pentagons of the four adjoined pentagons. The C_{2v}:4*mbr* isomer shows two intensive peaks in the region of the C−C stretching mode (1459 and 1468 cm^{-1}). Both of the two peaks correspond to the stretching of the C−C bonds of adjoined hexagons except for the hexagons surrounding the square. Both of the two nonclassical isomers (C_s:7*mbr* and C_{2v}:4*mbr*) have weak oscillator strength (the maximal values are 16.00 km/mol and 15.44 km/mol, respectively) among breathing modes. It would be worthwhile to mention that the C_1:1077 has weaker IR intensity, and the intensities of the peaks of breathing modes are stronger than those of the stretching modes in C_1:1077. In addition, the other two classical isomers (C_2:0032 and C_1:0899) possess similar IR spectra as shown in Figure 3. Nevertheless, the IR spectra of C_1:0899 is different from C_2:0032 in the region around 1000 cm^{-1}. There are two intensive peaks (950 cm^{-1} and 1012 cm^{-1}) in this region for C_1:0899. Both of the two peaks correspond to the expanding of hexagons. These simulated IR spectra should be useful to identify these C_{62} isomers.

TABLE 2: NICS(0) Values (in ppm) of Some Rings in the Three Most Stable Isomers of C_{62} Fullerene[a]

C_s:7mbr		C_{2v}:4mbr		C_2:0032	
no.	NICS(0)	no.	NICS(0)	no.	NICS(0)
7	−6.5	6[a]	−8.5	5[b]	13.0
5[c]	11.7	6[a]	−8.5	5[b]	13.0
5[b]	13.3	6[a]	−4.7	5[c]	16.0
5[b]	13.3	6[a]	−4.7	5[c]	16.0
5[a]	29.3	4	28.9	5[a]	24.0
5[a]	29.3			5[a]	24.0
center	−0.5		−5.6		2.0

[a] The numbers 4, 5, 6, and 7 in the columns labeled "no." refer to the square, pentagon, hexagon, and heptagon, respectively. The superscript represents the rings as shown in Figure 1.

3.4. Aromaticity and Chemical Activity. NICS can help to predict the local aromaticity in C_{62} fullerene. Schleyer et al. proposed using absolute magnetic shielding computed at the ring center as a criterion to measure aromaticity of cyclic structures, referred to as NICS: Significantly negative (i.e., magnetically shielded) NICS values in the interior positions of rings or cages indicate the presence of induced diatropic ring currents or "aromaticity", whereas positive values (i.e., deshielded) denote paratropic ring currents or "antiaromaticity".[30] The NICS values at the center [NICS(0)] of every ring as well as the NICS 1 Å above [NICS(1)] and below [NICS(−1)] each ring center of the three most stable C_{62} isomers are predicted. All data is listed in Table 2 and Supporting Information.

The heptagon is an aromatic ring because it possesses the most negative value of NICS(0) (−6.5 ppm) among all the rings of C_s:7*mbr*. Five pentagons with large positive values of NICS(0) are all adjacent to the heptagon. The middle two of the chain of four pentagons have the largest value of NICS(0) (29.3 ppm). All 13 pentagons in C_s:7*mbr* are antiaromatic rings with positive values of NICS(0). However, only 10 of 19 hexagons have a negative NICS(0) value. The small value of NICS (−0.5 ppm) at the cage center of C_s:7*mbr* suggests that the isomer is nonaromatic.

The square ring in C_{2v}:4*mbr* is antiaromatic because of its positive value of NICS(0) (28.9 ppm). All 10 pentagons have a positive NICS(0) value. The four hexagons surrounding the square are nonplanar, and they have a positive NICS(0) value (2.3 ppm) which is opposite to the value (−2.5 ppm)[31] for hexagons in C_{60}. C_{2v}:4*mbr* displays aromatic character with an NICS(0) of −5.6 ppm at the cage center. In addition, the six pentagons with large positive values of NICS(0) are three pairs

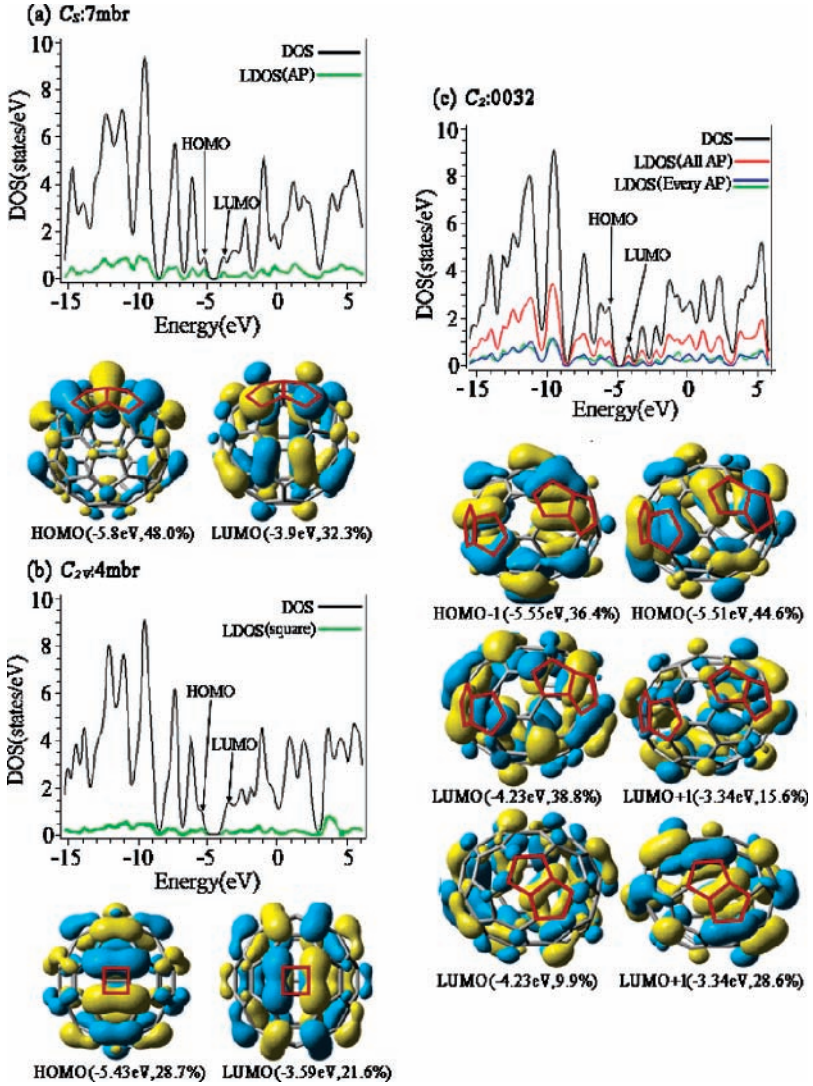

Figure 4. Total density of states (DOS), the local density of states (LDOS), and some frontier molecular orbits (FMOs) of C_{62} (a, C_s:7*mbr*; b, C_{2v}:4*mbr*; c, C_2:0032). The two values in parentheses of the FMOs represent the energy levels (in eV) and the contribution of electron density from the highlighted regions, respectively. The LDOSs refer to the heptagon and the square in C_s:7*mbr* and C_{2v}:4*mbr*, respectively. In C_2:0032, "LDOS (All AP)" represents the contributions of adjacent pentagons (AP) marked with a, b, and c in Figure 1. The blue line of "LDOS (Every AP)" refers to the contributions of the AP marked with a and b, and the green line refers to the AP marked with c.

of adjacent pentagons in isomer C_2:0032. Therefore, the six pentagons are antiaromatic rings. The NICS value of the cage center in C_2:0032 is 2.0 ppm.

To get an insight into the chemical activity of the first three most table isomers of C_{62}, we analyze several HOMOs, LUMOs, and the local density of states (LDOS) of some regions. As to C_s:7*mbr*, the contribution of electron density from the middle two adjacent pentagons among these four surrounding the heptagon is large in the HOMO and LUMO (see Figure 4a). The contribution from these two adjacent pentagons to the HOMO and LUMO is 48.0% and 32.3%, respectively. However, these two pentagons offer less contribution to the HOMO-1(7.0%) and HOMO-2(7.1%). On the basis of the analyses above, these two adjacent pentagons should possess high chemical activity. For C_{2v}:4*mbr*, the contribution of electron density from the square to the HOMO and LUMO [see Figure 4b] are 28.7% and 21.6%, respectively, suggesting that the square in C_{2v}:4*mbr* should possess high chemical activity. There are two kinds (total three pairs) of symmetrically distinct adjacent pentagons in C_2:0032. The three pairs of adjacent pentagons have large contributions to both the HOMO and LUMO (48.7% and 48.8%, respectively) (see Figure 4c). The adjacent pentagon pair (a + b in Figure 1) has a large contribution to the HOMO and LUMO (22.8% and 19.3%, respectively). The contribution from another adjacent pentagon marked with c of C_2:0032 (See Figure 1) to the HOMO and LUMO (3.0% and 9.9%, respectively) is small. However, its contribution to the LUMO+1 is large (28.6%), and the contribution to the HOMO-1 is larger than that to the HOMO. From the analyses above, the two pairs of symmetrically identical adjacent pentagons (a + b) should possess high chemical activity due to their large contributions to the HOMO and LUMO in C_2:0032.

3.5. Electronic Spectra and Nonlinear Optical Properties. The electronic spectra reflects the electronic structure of a system and it helps to identify the structure of the system in experiments. Theoretical studies of NLO properties help to reveal structure−property relationships and search promising NLO materials. In this work, ZINDO/SOS is utilized to predict the electronic spectra and the hyperpolarizabilities for the five most stable C_{62} isomers.

Three different external field frequencies ω (ω = 0.6491, 1.1653, and 2.3305 eV) are adopted to evaluate the second-order hyperpolarizability of the five most stable isomers, and

TABLE 3: Predicted Isotropically Averaged Values of the Third-Order Polarizability $\langle\gamma\rangle$ of C_{62} Using INDO/SCI with the SOS Model (units: 10^{-34} esu) in the Presence of External Field Frequencies ω[a]

	$\gamma(-3\omega;\omega,\omega,\omega)$			$\gamma(-2\omega;\omega,\omega,0)$			$\gamma(-\omega;\omega,\omega,-\omega)$		$\gamma(0;-\omega,\omega,0)$	
	0.0[b]	0.6491	1.1653	0.6491	1.1653	0.6491	1.1653	2.3305	0.6491	1.1653
C_{60}	13.01	15.18		14.00	16.82	13.65	15.23	26.17	13.33	
$C_{62}(C_s$:7*mbr*)	16.79	20.39	29.26	18.56	3.015×10^4	18.02	27.33	1.974×10^9	17.39	18.95
$C_{62}(C_2$:4*mbr*)	16.00	22.31	138.03	17.66	23.54	17.02	19.79	178.65	16.51	17.80
$C_{62}(C_2$:0032)	23.40	20.66	37.60	41.93	28.00	34.92	76.59	573.74	28.23	33.75
$C_{62}(C_1$:0899)	30.19	60.79	48.63	146.66	25.52	5952.90	56.96	291.93	281.11	31.03
$C_{62}(C_1$:1077)	18.74	12.33	28.21	15.55	23.47	23.34	39.21	223.49	20.76	21.98

[a] C_{60} data are obtained from ref 24. [b] ω/eV.

the predicted values are listed in Table 3 and are compared with the corresponding values of C_{60} predicted at the same level of theory.[24] All γ values [except for the $\gamma(-3\omega;\omega,\omega,\omega)$ (ω = 1.1653 eV) of C_1:1077] of the five most stable C_{62} isomers at different external field frequencies are larger than those of C_{60}.[24] The dc-electric field induced second harmonic generation (DC-EFISHG) $\gamma(-2\omega;\omega,\omega,0)$ at ω=1.1653 eV for the C_s:7*mbr* isomer is remarkable, being about 1793 times larger than that of C_{60}. It should be mentioned that there are large values of the intensity-dependent refractive index (IDRI) at ω=2.3305 eV for the five most stable isomers, whose enhancements are due to resonance with the external field. Take the C_2:0032 isomer for example: The IDRI (5.74×10^{-32} esu) is 22 times larger than the static γ. The IDRI, $\gamma(-\omega;\omega,\omega,-\omega)$ (ω = 2.3305 eV) of C_s:7*mbr* due to resonance with external field, which is 7.55×10^7 times larger than that of C_{60},[24] suggests that C_s:7*mbr* might be a potential NLO candidate.

To get an insight into the evolution of the average γ, $\langle\gamma\rangle$, with electron excitations, the static second-order hyperpolarizability and the UV−vis spectra are plotted in Figure 5. The static second-order hyperpolarizability of the five stable isomers increases gradually with electron excitations up to 10 eV as illustrated in Figure 5, and it can be mainly divided into four regions, i.e., 0−4.0, 4.0−6.0, 6.0−8.0, and 8.0−10.0 eV. Take C_1:0899 for example: The $\langle\gamma\rangle$ increases about 18.6×10^{-34} esu from the contribution of the electron excitation from 4.0 to 6.0 eV, and it increases about 5.7×10^{-34} esu in the region from 8.0 to 10.0 eV. The static γ of C_1:0899 converges to 30.19 $\times 10^{-34}$ esu, which is about 132% lager than that of C_{60}. The second-order hyperpolarizabilities of the other three isomers are presented in Table 3. These values are also larger than those of C_{60}.

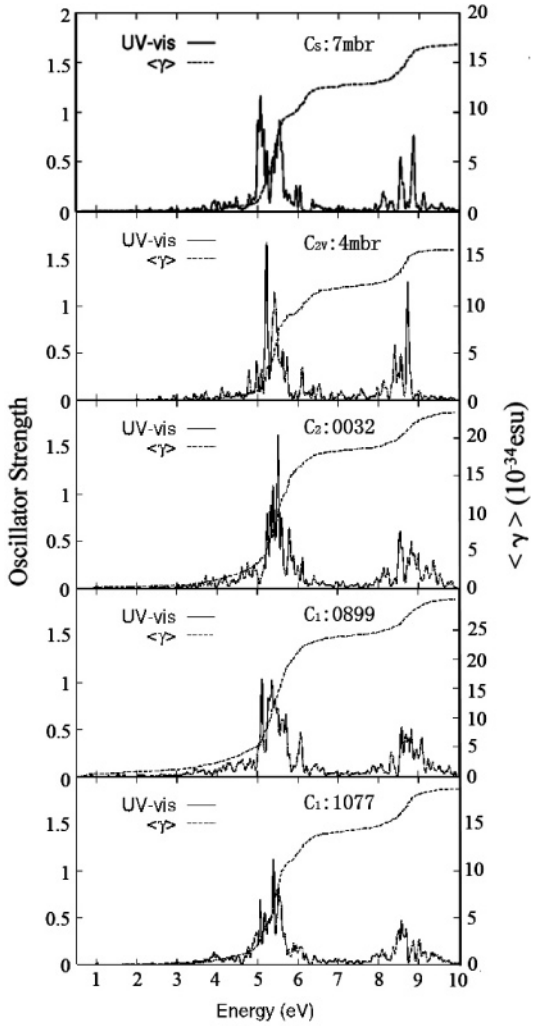

Figure 5. Electronic spectra of the five most stable C_{62} isomers predicted by ZINDO/SCI, and the isotropically averaged static second-order hyperpolarizability $\langle\gamma\rangle$ predicted by ZINDO/SOS. The UV plot is broadened by 0.05 eV.

4. Conclusions

Using PM3 together with SVWN, HCTH, and B3LYP, we have investigated all the C_{62} classical isomers and four nonclassical isomers systematically. C_s:7*mbr* with a chain of four adjacent pentagons surrounding a heptagon is predicted to possess the lowest energy, and another nonclassical isomer, C_{2v}:4*mbr* with a square, is the second most stable isomer. The most stable classical isomer is C_2:0032 with three pairs of adjacent pentagons. The relative stability under the interisomeric thermodynamic equilibrium has been evaluated in terms of Gibbs function. C_s:7*mbr* prevails in a wide temperature range.

Simulated IR spectra for the five most stable isomers are also presented, and the most stable isomer C_s:7*mbr* exhibits the most intensive peak in the frequency range. The peak corresponds to a breathing mode, while the C_1:0899 isomer shows several intensive peaks corresponding to the stretching of C−C bonds. The formation of a heptagon by insertion of a C2-unit into C_{60} makes the new heptagon aromatic and makes the middle two of the chain of four pentagons possess high chemical reactivity. The square formed by insertion of a C2-unit into C_{60} possesses high chemical reactivity in C_{2v}:4*mbr*. The adjacent pentagons are predicted to possess high chemical activity in C_2:0032. In addition, ZINDO/SOS is utilized to determine the hyperpolarizabilities for the five most stable C_{62} isomers. The static second-order hyperpolarizabilities of C_{62} isomers exceed that of C_{60}. Furthermore, the intensity-dependent refractive index $\gamma(-\omega;\omega,\omega,-\omega)$ at ω = 2.3305 eV is very large for C_s:7*mbr*.

Note Added in Proof. After we submitted this manuscript, Shao et al.[32] reported a search for the most stable fullerenes (C_{38}−C_{80} and C_{112}−C_{120}) with PBE1PBE/6-311G(d)//DFTB.

Acknowledgment. This work is supported by the National Nature Science Foundation of China (20473031). W.Q.T. thanks the start-up fund from Jilin University.

Supporting Information Available: The value of NICS(0), NICS(1), and NICS(−1) (in ppm) of rings in the three most stable isomers (C_s:7*mbr*, C_{2v}:4*mbr*, and C_2:0032) of C_{62} fullerene. This material is available free of charge via the Internet at http://pubs.acs.org.

References and Notes

(1) Kroto, H. W.; Heath, J. R.; O'brien, S. C.; Curl, R. F.; Smalley, R. E. *Nature* **1985**, *318*, 162.

(2) Krätschmer, W.; Lamb, L. D.; Fostiropoulos, K.; Huffman, D. R. *Nature* **1990**, *347*, 354.

(3) Shinar, J.; Vardeny, Z. V.; Kafafi, Z. H. *Optical and Electronic Properties of Fullerenes and Fullerene-Based Materials*; Marcel Dekker, Inc.: New York, 2000.

(4) Eklund, P. C.; Rao, A. M. *Fullerene Polymers and Fullerene Polymer Composites*; Springer-Verlag: Berlin, 1999.

(5) Fowler, P. W.; Manolopoulos, D. E. *An Atlas of Fullerenes*; Oxford University Press: New York, 1995.

(6) Kroto, H. W. *Nature* **1987**, *329*, 529.

(7) Schmalz, T. G.; Seitz, W. A.; Klein, D. J.; Hite, G. E. *J. Am. Chem. Soc.* **1988**, *110*, 1113.

(8) Ayuela, A.; Fowler, P. W.; Mitchell, D.; Schmidt, R.; Seifert, G.; Zerbetto, F. *J. Phys. Chem.* **1996**, *100*, 15634.

(9) Hernandez, E.; Ordejon, P.; Terrones, H. *Phys. Rev. B* **2001**, *193*, 193403.

(10) Fowler, P. W.; Heine, T.; Mitchell, D.; Orlandi, G.; Schmidt, R.; Seifert, G.; Zerbetto, F. *J. Chem. Soc., Faraday Trans.* **1996**, *92*, 2203.

(11) Albertazzi, E.; Domene, C.; Fowler, P. W.; Heine, T.; Seifert, G.; Alsenoy Van, C.; Zerbetto, F. *Phys. Chem. Chem. Phys.* **1999**, *1*, 2913.

(12) Qian, W. Y.; Bartberger, M. D.; Pastor, S. J.; Houk, K. N.; Wilkins, C. L.; Rubin, Y. *J. Am. Chem. Soc.* **2000**, *122*, 8333.

(13) Qian, W. Y.; Chuang, S. C.; Amador, R. B.; Jarrosson, T.; Sander, M.; Pieniazek, S.; Khan, S. I.; Rubin, Y. *J. Am. Chem. Soc.* **2003**, *125*, 2066.

(14) Hou, J. Q.; Kang, H. S. *J. Comput. Chem.* **2007**, *28*, 1417.

(15) Campbell, E. E. B.; Fowler, P. W.; Mitchell, D.; Zerbetto, F. *Chem. Phys. Lett.* **1996**, *250*, 544.

(16) Brinkmann, G.; Dress, A. W. M. *J. Algorithm*, **1997**, *23*, 345. For a completely new version of CaGe, see http://www.mathematik.uni-bielefeld.de/∼CaGe.

(17) Stewart, J. J. P. *J. Comput. Chem.* **1989**, *10*, 209.

(18) Boese, A. D.; Handy, N. C. *J. Chem. Phys.* **2001**, *114*, 5497.

(19) Vosko, S. H.; Wilk, L.; Nusair, M. *Can. J. Phys.* **1980**, *58*, 1200.

(20) Becke, A. D. *J. Chem. Phys.* **1993**, *98*, 5648.

(21) Tian, W. Q.; Feng, J.-K.; Wang, Y. A.; Aoki, Y. *J. Chem. Phys.* **2006**, *125*, 094105.

(22) Frisch, M. J.; Trucks, G. W.; Schlegel, H. B.; Scuseria, G. E.; Robb, M. A.; Cheeseman, J. R.; Zakrzewski, V. G.; Montgomery, J. A., Jr.; Stratmann, R. E.; Burant, J. C.; Dapprich, S.; Millam, J. M.; Daniels, A. D.; Kudin, K. N.; Strain, M. C.; Farkas, O.; Tomasi, J.; Barone, V.; Cossi, M.; Cammi, R.; Mennucci, B.; Pomelli, C.; Adamo, C.; Clifford, S.; Ochterski, J.; Petersson, G. A.; Ayala, P. Y.; Cui, Q.; Morokuma, K.; Malick, D. K.; Rabuck, A. D.; Raghavachari, K.; Foresman, J. B.; Cioslowski, J.; Ortiz, J. V.; Stefanov, B. B.; Liu, G.; Liashenko, A.; Piskorz, P.; Komaromi, I.; Gomperts, R.; Martin, R. L.; Fox, D. J.; Keith, T.; Al-Laham, M. A.; Peng, C. Y.; Nanayakkara, A.; Gonzalez, C.; Challacombe, M.; Gill, P. M. W.; Johnson, B. G.; Chen, W.; Wong, M. W.; Andres, J. L.; Head-Gordon, M.; Replogle, E. S.; Pople, J. A. *Gaussian 03, revision C.02*; Gaussian, Inc.: Wallingford, CT, 2004.

(23) Slanina, Z. *Int. Rev. Phys. Chem.* **1987**, *6*, 251.

(24) Gu, F. L.; Chen, Z.; Jiao, H. J.; Tian, W. Q.; Aoki, Y.; Thief, W.; Schleyer, P. v. R. *Phys. Chem. Chem. Phys.* **2004**, *6*, 4566. Some earlier works on the second hyperpolarizabilities on fullerenes are as follows: (a) Fanti, M.; Orlandi, G.; Zerbetto, F. *J. Am. Chem. Soc.* **1995**, *117*, 6101. (b) Li, J.; Feng, J.-K.; Sun, J. *Chem. Phys. Lett.* **1993**, *203*, 560. (c) Gisbergen, S. J. A. van; Snijders, J. G.; Baerends, E. J. *Phys. Rev. Lett.* **1997**, *78*, 3097 and references therein.

(25) Feng, J. K.; Ren, A. M.; Tian, W. Q.; Ge, M. F.; Li, Z. R.; Sun, C. C.; Zheng, X. H.; Zener, M. C. *Int. J. Quantum Chem.* **2000**, *76*, 23.

(26) Tajima, Y.; Takeuchi, K. *J. Org. Chem.* **2002**, *267*, 1696.

(27) Ridley, J.; Zerner, M. C. *Theor. Chim. Acta* **1973**, *111*, 32.

(28) Orr, B. J.; Ward, T. F. *Mol. Phys.* **1971**, *513*, 20.

(29) Li, J.; Feng, J. K. *J. Chem. Phys. Lett.* **1993**, *203*, 560.

(30) Schleyer, P. v. R.; Manoharan, M.; Wang, Z. X.; Kiran, B.; Jiao, H.; Puchta, R.; Hommes, N. J. R. v. E. *Org. Let.* **2001**, *3*, 2465.

(31) Chen, Z. F.; King, R. B *Chem. Rev.* **2005**, *105*, 3613.

(32) Shao, N.; Gao, Y.; Zeng, X. C. *J. Phys. Chem. C* **2007**, DOI-(10.1021/jp0701082).